

- (1968).
- (38) G. K. Pagenkopf and D. W. Margerum, *J. Am. Chem. Soc.*, **90**, 6963 (1968).
- (39) H. Hauer, G. R. Dukes, and D. W. Margerum, *J. Am. Chem. Soc.*, **95**, 3515 (1973).
- (40) J. C. Cooper, L. F. Wong, D. L. Venezky, and D. W. Margerum, *J. Am. Chem. Soc.*, **98**, 7560 (1974).
- (41) C. E. Bannister, D. W. Margerum, J. M. T. Raycheba, and L. F. Wong, *Faraday Symp. Chem. Soc.*, No. 10, 78 (1975).
- (42) H. L. Schlüter and G. Gliemann, "Basic Principles of Ligand Field Theory," Wiley-Interscience, New York, N.Y., 1969, p 78.
- (43) E. J. Billo, *Inorg. Nucl. Chem. Lett.*, **10**, 613 (1974).
- (44) R. Skochdopole and S. Chaberek, *J. Inorg. Nucl. Chem.*, **11**, 222 (1959).
- (45) J. Shankar and B. C. DeSouza, *Aust. J. Chem.*, **16**, 1119 (1963).
- (46) L. H. Sutcliffe and J. R. Weber, *Trans. Faraday Soc.*, **52**, 1225 (1956).
- (47) E. T. Gray, Jr., R. W. Taylor, and D. W. Margerum, to be submitted for publication.
- (48) D. H. McDaniel and H. C. Brown, *J. Org. Chem.*, **23**, 420 (1958).
- (49) S. J. Leach, G. Nemethy, and H. Scheraga, *Biopolymers*, **4**, 369 (1966).
- (50) T. Peters, Jr., and F. A. Blumenstock, *J. Biol. Chem.*, **242**, 1574 (1967).
- (51) E. Breslow, *J. Biol. Chem.*, **239**, 3252 (1964).
- (52) W. T. Shearer, R. A. Bradshaw, F. R. N. Gurd, and T. Peters, Jr., *J. Biol. Chem.*, **242**, 5451 (1967).
- (53) R. A. Bradshaw, W. T. Shearer, and F. R. N. Gurd, *J. Biol. Chem.*, **243**, 3817 (1968).
- (54) D. C. Weatherburn, E. J. Billo, J. P. Jones, and D. W. Margerum, *Inorg. Chem.*, **9**, 1557 (1970).
- (55) O. Yamauchi, Y. Nakao, and A. Nakahara, *Bull. Chem. Soc. Jpn.*, **46**, 2119 (1973).
- (56) H. C. Freeman, ref 29, Chapter 4, p 145.
- (57) F. Akhtar, D. M. L. Goodgame, M. Goodgame, G. W. Rayner-Canham, and A. C. Skapski, *Chem. Commun.*, 1389 (1968).
- (58) L. F. Wong and D. W. Margerum, submitted for publication.
- (59) F. Basolo and R. G. Pearson, "Mechanisms of Inorganic Reactions", 2nd ed, Wiley, New York, N.Y., 1967, p 70.
- (60) J. M. Tsangaras and R. B. Martin, *J. Am. Chem. Soc.*, **92**, 4255 (1970).
- (61) G. F. Bryce, *J. Phys. Chem.*, **70**, 3549 (1966).
- (62) I. M. Procter, B. J. Hathaway, and P. Nichols, *J. Chem. Soc. A*, 1678 (1968).
- (63) C. K. Jørgensen, "Oxidation Numbers and Oxidation States", Springer Verlag, Berlin, 1969, p 57.
- (64) F. P. Bossu and D. W. Margerum, *J. Am. Chem. Soc.*, **98**, 4003 (1976).
- (65) F. P. Bossu and D. W. Margerum, *Inorg. Chem.*, in press.
- (66) G. A. Hamilton, R. D. Libby, and C. R. Hartzell, *Biochem. Biophys. Res. Commun.*, **55**, 333 (1973).
- (67) G. R. Dyrkacz, R. D. Libby, and G. A. Hamilton, *J. Am. Chem. Soc.*, **98**, 626 (1976).
- (68) R. P. Bereman, R. S. Giordano, D. J. Kosman, M. J. Ettinger, and R. E. Weiner, American Chemical Society Meeting, New York, N.Y., 1976.
- (69) L. Cleveland, R. E. Coffman, P. Coon, and L. Davis, *Biochemistry*, **14**, 1108 (1975).

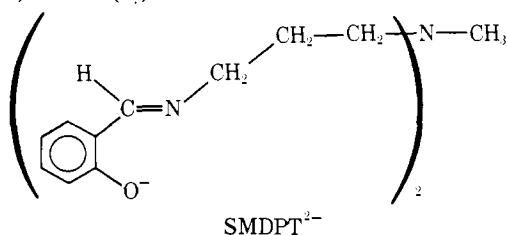
## Ambidentate Nature of the Imidazole Ring System

Benjamin S. Tovrog and Russell S. Drago\*

Contribution from the William A. Noyes Laboratory, University of Illinois, Urbana, Illinois 61801. Received June 3, 1976

**Abstract:** In this article, we present additional support for our earlier claim that the imidazole ring system can bind through the amine nitrogen. The isotropic shifts and the line widths of *N*-methylimidazole coordinated to Co(SMDPT) are consistently interpreted in terms of coordination at this site.

Our earlier report on the ambidentate nature of imidazole<sup>1</sup> caused great surprise<sup>2</sup> because the amine nitrogen was supposed to be like that in pyrrole, which is claimed not to be basic. In this article, we shall present further evidence for the ambidentate nature of this donor. In view of the limited solubility of the metal complexes used in the earlier work and the potential complications from the ability of imidazole to hydrogen bond, we decided that an even more convincing case could be made for the ambidentate nature of this ring system by examining the NMR spectra of *N*-methylimidazole (*N*-MeIm) coordinated to the complexes M(SMDPT), where M is Ni(II) and Co(II) and SMDPT<sup>2-</sup> is shown below.



We report not only the isotropic shifts of the complexes, but the line widths of the resonances as well. In either the very fast or stopped exchange regions, the line width is often related to the distance of the observed nucleus from the metal center. This data (along with full details of the experimental procedure) shows a different mode of bonding for *N*-MeIm to the cobalt(II) and nickel(II) complexes of SMDPT.

### Experimental Section

M(SMDPT), M = Ni(II) and Co(II), were prepared by reported procedures.<sup>3</sup> *N*-Methylimidazole was obtained from Aldrich Chemical

Co. and fractionally distilled over CaH<sub>2</sub> at 10-mm pressure, with only the middle fraction retained. Samples for NMR were prepared in volumetric flasks in an inert atmosphere dry box with dry deoxygenated CDCl<sub>3</sub> as solvent utilizing tetramethylsilane (Me<sub>4</sub>Si) as an internal standard. NMR tubes were equipped with tight-fitting caps and wrapped with Parafilm to exclude oxygen. The proton NMR spectra were measured either with a JOELCO-C-60H high resolution NMR spectrometer equipped with a JES-VT-2 temperature controller, or a Varian Associates HA-100 NMR spectrometer operating in the field sweep mode equipped with a temperature control unit. In the HA-100 spectra, Me<sub>4</sub>Si was utilized as the lock signal. The probe temperatures were measured to ±1.0 °C using either a copper-constantan thermocouple or by measuring the NMR spectrum of methanol. Solution magnetic moments were determined by the Evans method, monitoring the Me<sub>4</sub>Si signal. Electron spin resonance spectra were collected on a Varian Model E-9 spectrometer equipped with a Hewlett-Packard frequency counter. Cooling was provided by cold nitrogen gas. The field was calibrated using a Varian weak pitch sample.

### Results and Discussion

**Nature of the Adducts Formed.** Co(SMDPT) (**1**) and Ni(SMDPT) (**2**) are five-coordinate high-spin d<sup>7</sup> and d<sup>8</sup> complexes, respectively. The magnetic moment of **1** is 4.28 μ<sub>B</sub> in CH<sub>2</sub>Cl<sub>2</sub> solution and 4.29 μ<sub>B</sub> in the solid. Though the structure of **1** is not known, **2** has been examined and found to possess a distorted trigonal bipyramidal structure.<sup>4,5</sup> The similarity in spectral properties between **1** and **2** suggests similar structures. Infrared spectra are virtually identical, and their paramagnetic NMR spectra are also very similar. In **2**, all the aromatic ring protons are split into two equally intense resonances,<sup>5</sup> due to different orientations of the *N*-CH<sub>3</sub> group with respect to each phenyl ring.<sup>6</sup> The observation of a similar

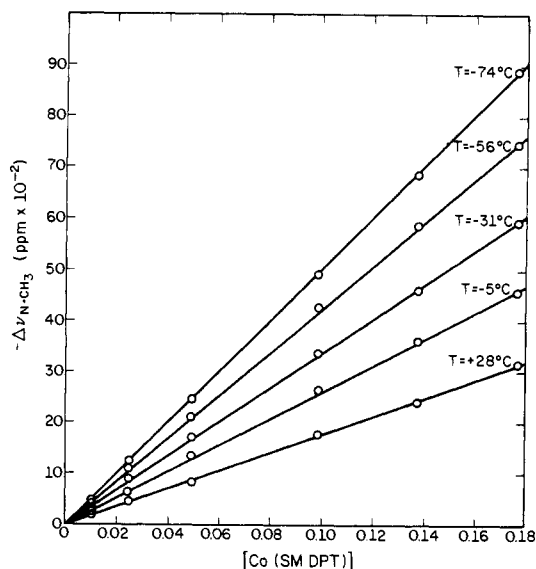


Figure 1. Isotropic shift of the  $N$ -CH<sub>3</sub> resonance of  $N$ -methylimidazole in CDCl<sub>3</sub> solutions containing Co(SMDPT) at various temperatures.

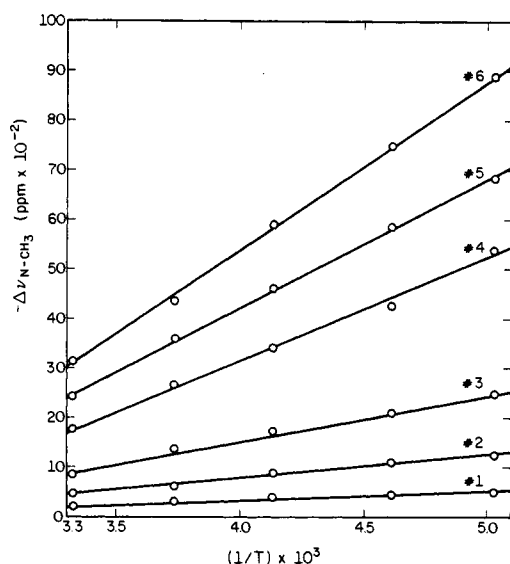


Figure 2. Temperature dependence of the isotropic shift of  $N$ -methylimidazole in CDCl<sub>3</sub> solutions containing Co(SMDPT).

"doubling" in **1** below 0 °C suggests<sup>7</sup> a structure similar to that of **2**.

Unlike most five-coordinate cobalt(II) complexes that result from adduct formation of a Lewis base with four-coordinate, planar complexes, **1** will form high-spin adducts with a variety of nitrogen donor Lewis bases. The formation constants are very small, making isolation of the adducts impossible. Distinct visible spectral features of **1** are obscured by an intense charge-transfer band, but a low intensity peak at 6800 Å ( $\epsilon$  25.8) can be discerned. Changes in this peak occur with the addition of Lewis bases, but the shifts are too small to allow accurate calculation of equilibrium constants. Adduct formation is further verified by the paramagnetic NMR shifts observed in Table I for CH<sub>3</sub>CN and (CH<sub>3</sub>)<sub>2</sub>NCN adducts. The adducts are in fast exchange with free base at room temperature and exchange cannot be slowed in the proton resonances down to -100 °C.  $N$ -MeIm protons exhibit observable isotropic shifts in solutions containing **1** and Figure 1 shows the linear dependence of the concentration of **1** vs. the  $N$ -CH<sub>3</sub> chemical shift. Utilizing a constant base concentration, the plot should

Table I. NMR Chemical Shifts of Base Protons<sup>a</sup> in Solutions Containing Co(SMDPT)

[CH <sub>3</sub> CN]	[Co(SMDPT)]	$-\nu_{\text{CH}_3}$	$T, ^\circ\text{C}$
0.450	0.00	2.00	25.0
0.360	0.066	2.10	25.0
0.277	0.127	2.22	25.0
0.212	0.175	2.26	25.0
0.156	0.216	2.34	25.0
0.156	0.216	2.53	2.0
0.156	0.216	2.92	-33.0
0.156	0.216	3.12	-66.0

[(CH <sub>3</sub> ) <sub>2</sub> NCN]	[Co(SMDPT)]	$-\nu_{\text{CH}_3}$	$T, ^\circ\text{C}$
0.424	0.00	2.85	25.0
0.359	0.030	2.87	25.0
0.275	0.087	2.90	25.0
0.198	0.132	2.95	25.0
0.139	0.166	2.97	25.0
0.105	0.186	3.00	25.0
0.105	0.186	3.18	-2.0
0.105	0.186	3.20	-21.0
0.105	0.186	3.23	-40.0
0.105	0.186	3.30	-66.0

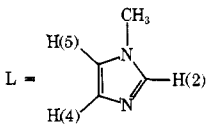
<sup>a</sup> Chemical shifts in parts per million downfield from Me<sub>4</sub>Si.

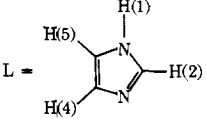
be linear if the concentration of free base is much greater than the concentration of the base adduct in solution. The linearity of the plot up to a concentration ratio of [1]/[ $N$ -MeIm] of 2.25 underscores the small equilibrium constant. The solubility of **1** and low signal intensity of  $N$ -MeIm protons in the presence of **1** prevents investigation of larger cobalt/base ratios. The isotropic shift of the  $N$ -CH<sub>3</sub> group shows a linear  $1/T$  dependence for all solutions studied (Figure 2). Similar well-behaved plots exist for interaction of  $N$ -MeIm with **2**, see Figures 3 and 4.<sup>9</sup> Extrapolation of the linear plots in Figures 2 and 4 to  $1/T = 0$  reveal nonzero intercepts. Zero field splittings in these  $S > 1/2$  systems can cause such behavior.<sup>8</sup> Additionally, the temperature dependence of the coordination of  $N$ -MeIm can be a contributor to the nonzero intercept.<sup>8</sup>

Magnetic moment determinations of solutions containing **1** in the presence of added base all show high-spin character, but in view of the small equilibrium constants for adduct formation, this is not definitive evidence for the high-spin nature of these adducts. The best evidence for the high-spin character of the base adducts comes from ESR. Zero field splitting within the quartet ground state of **1** gives rise to a short electron spin relaxation time and an accompanying broad ESR signal. The spectrum at -160 °C in a 50/50 v/v CH<sub>2</sub>Cl<sub>2</sub>/toluene glass is a broad, featureless signal centered at  $g = 4.3$  with a half width of approximately 1000 G. Solutions including the bases listed in Table I ([base]  $\sim$  1 M, [1]  $\sim$  0.3 M) give rise to similar high-spin signals. Though identification of separate signals from free and complexed **1** cannot be made due to the breadth of the resonances, the absence of low-spin signals which would occur in the vicinity of  $g = 2$  confirms the high-spin nature of these adducts.

**NMR Chemical Shifts.** The NMR isotropic shifts of various imidazole and  $N$ -CH<sub>3</sub> imidazole complexes studied here and others reported in the literature are summarized in Table II. One notes by examining the observed shifts for Ni(DPM)<sub>2</sub>L<sub>2</sub><sup>10</sup> and Ni(acac)<sub>2</sub>L<sub>2</sub> (Table II) that the expected  $\sigma$  delocalization pattern for this ligand coordinated to the pyridine type nitrogen involves a downfield shift of the 2, 4 and 5 ring protons. The  $N$ -CH<sub>3</sub> resonances undergo a slight upfield shift. This pattern of ring and methyl shifts is similar to that previously reported for 4-picoline complexes of nickel(II). Molecular orbital calculations on this system<sup>11,12</sup> supported a dominant  $\sigma$  delocal-

Table II. NMR Chemical Shifts of *N*-MeIm and Im Coordinated to Metal Ions and Complexes<sup>a</sup>

Complex				
	$\Delta\nu_{\text{H}(2)}$	$\Delta\nu_{\text{H}(4)}$	$\Delta\nu_{\text{H}(5)}$	$\Delta\nu_{\text{N-CH}_3}$
Co(dpm) <sub>2</sub> ·L <sub>2</sub> <sup>10</sup>	-100	-100	-100	23.3
Ni(dpm) <sub>2</sub> ·L <sub>2</sub> <sup>10</sup>			-130	6.6
Eu(dpm) <sub>3</sub> ·L <sup>10</sup>	-100	-88.3	-35.3	-38.2
Pr(dpm) <sub>3</sub> ·L <sup>10</sup>	100	93.2	46.6	33.2
Ni(acac) <sub>2</sub> ·L <sub>2</sub>	-100	-100	-73.5	12.4
Ni(SMDPT)·L <sup>b</sup>	-100	-100	-98.6	14.0
Co(SMDPT)·L <sup>b</sup>	100	616	-386	-909
Fe(TPP)L <sub>2</sub> <sup>+</sup> Cl <sup>-c</sup>	8.5	~-6.9	~-3.2	-17.2

Complex		
	$\Delta\nu_{\text{H}(2)}$	$\Delta\nu_{\text{H}(4,5)}$
FeL <sub>6</sub> <sup>2+ 14</sup>	-100	-162.7
CoL <sub>6</sub> <sup>2+ 14</sup>	-100	-161.8
NiL <sub>6</sub> <sup>2+ 14</sup>	-100	-110.0
Fe(TPP)L <sub>2</sub> <sup>+</sup> Cl <sup>-c, d</sup>	9.5 (28)	-9.7, -4.0 ( $\Delta\nu_{\text{H}(1)} = -2.0$ ) (8.2, 7.6) ( $\Delta\nu_{\text{H}(1)} = 9.6$ )

<sup>a</sup> All shifts normalized to  $\Delta\nu_{\text{H}(2)} = 100$  unless otherwise indicated; + refers to upfield shift, - to downfield shifts. <sup>b</sup> Shifts from the free ligand resonances obtained from solution no. 6 data for Co(SMDPT) and solution no. 4 data for Ni(SMDPT). The coordinated *N*-methylimidazole undergoes fast exchange with free base so all shifts have been normalized to  $\Delta\nu_{\text{H}(2)} = 100$ . For Co(SMDPT), see microfilm edition for complete tabulation of all chemical shifts. <sup>c</sup> J. D. Satterlee and G. N. LaMar, *J. Am. Chem. Soc.*, 98, 2804 (1976). TPP is an abbreviation for tetraphenylporphyrin. This is the reported isotropic shift value. <sup>d</sup> Values in parentheses result after factoring the dipolar contribution from the isotropic shift.

ization mechanism to account for the attenuating downfield shifts at the 2 and 3 positions and a small  $\pi$  delocalization contribution of opposite sign spin density to account for the upfield shift of the -CH<sub>3</sub> group. Since a restricted EHT molecular orbital calculation was involved, this  $\pi$  polarization was gauged by the coefficients of the filled  $\pi$  (or empty  $\pi^*$ ) orbital. In the unrestricted calculations, e.g., INDO, the polarization of filled  $\pi$  orbitals is built into the calculation and the upfield shift of the methyl from  $\sigma$  bonding to the lone pair is predicted<sup>13</sup> directly.

In the octahedral complexes of imidazole, one again observed downfield shifts in the ring protons for the iron(II), cobalt(II), and nickel(II) complexes. Averaging out of the dipolar (pseudo contact) contributions in systems of this sort has been discussed. Wicholas<sup>14</sup> has carried out an MO calculation of imidazole with a carbon atom substituted at the 3 position to generate a  $\sigma$  radical. The resulting spin densities correlate well with the observed ML<sub>6</sub><sup>2+</sup> shifts and substantiate the presumed  $\sigma$  mechanism. The low-spin complexes of Fe(TPP)Cl do not contain unpaired electrons in metal orbitals used in  $\sigma$  bonding to imidazole. Thus, one observes (after factoring out the dipolar contribution) a  $\pi$  delocalization pattern of isotropic shifts for an imine-coordinated nitrogen.

The imidazole complexes with the europium and praseodymium chelates Eu(dpm)<sub>3</sub> and Pr(dpm)<sub>3</sub> have a proton isotropic shift pattern that is dominated by the dipolar contribution.<sup>15</sup> The sign of the isotropic shift changes with metal variation from Eu to Pr because of differences in the *g* tensor anisotropy of the two complexes. Such shifts are dependent on the distance of the nucleus from the metal center as well as the

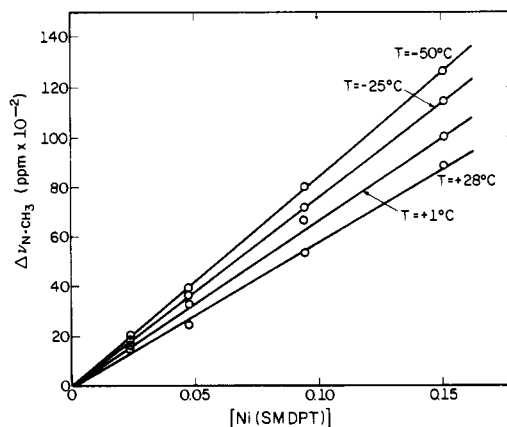


Figure 3. Isotropic shift of the *N*-CH<sub>3</sub> resonance of *N*-methylimidazole solutions containing Ni(SMDPT) at various temperatures.

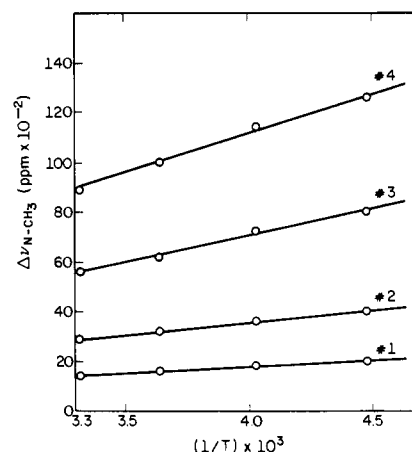
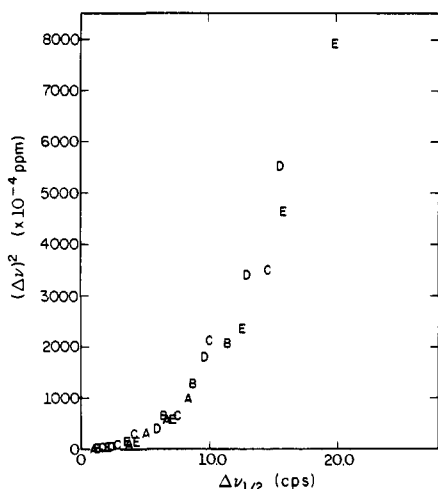


Figure 4. Temperature dependence of the isotropic shift of *N*-methylimidazole in solutions containing Ni(SMDPT).

angle the metal-nucleus vector makes with the magnetic *z* axis. Coordination through the imine nitrogen in these complexes is indicated by the larger H(2) and H(4) shifts relative to H(5) and the *N*-CH<sub>3</sub> group.

The similarity in the observed isotropic shifts for the cobalt(II) and nickel(II) complexes that are bound to the "pyridine type" nitrogen are expected on the basis of the results reported by Bertini and Gatteschi.<sup>16</sup> They observed similar contact shift patterns for pyridine, bipyridyl, phenanthroline, and naphthyridine type ligands with cobalt(II) and nickel(II) complexes of varying geometries and coordination numbers. They interpreted this similarity to the dominance of a predominantly  $\sigma$  delocalization mechanism in the bonding of these ligands to the metals. When coordination of imidazole occurs at the pyridine nitrogen, one would thus expect similar patterns of isotropic shifts for the cobalt(II) and nickel(II) complexes from a dominant  $\sigma$ -delocalization effect. (Often the dipolar contribution parallels the proton  $\sigma$ -delocalization pattern as can be seen for the ring protons in Table II.)

If coordination of **1** took place through N(3), all of the above results would lead one to expect a shift pattern similar to the complexes listed in Table II, i.e., large downfield shifts in H(2,4,5) and a smaller upfield shift in the *N*-CH<sub>3</sub> protons. Such a shift pattern is not observed for **1**. The observed ring proton shifts are all smaller than the *N*-CH<sub>3</sub> shift and exhibit both upfield and downfield shifts. In view of the variety of complexes listed in Table II, which show similar shift patterns for imine nitrogen coordination, these results suggest that a different mode of binding is involved in the *N*-MeIm adduct of **1**.



**Figure 5.** A plot of  $(\Delta\nu_{CH_3})^2$  vs.  $\Delta\nu_{1/2}$  for the  $N$ - $CH_3$  resonance of  $N$ -methylimidazole in solutions containing Co(SMDPT). The A points are derived from solution 2 at the five temperatures studied; similarly, B, C, D, and E are derived from data of solutions 3, 4, 5, and 6.

It is known in various alkylamine complexes of nickel(II) that the protons on the  $\alpha$ -carbon exhibit downfield shifts.<sup>17</sup> This trend persists in complexes **1** and **2** where the  $N$ - $CH_3$  group of the pentadentate ligand is shifted downfield 120 and 78.3 ppm,<sup>5</sup> respectively. The large downfield shift of the  $N$ - $CH_3$  resonance of  $N$ -MeIm is expected if coordination of **1** occurs at the N(1) donor of  $N$ -methylimidazole. With coordination at the  $N$ - $CH_3$ , unpaired spin can be delocalized directly into the  $\pi$  system as has been reported for benzylamine.<sup>18</sup> Such an effect would place unpaired electron density directly into the " $\pi$  system" and a very different isotropic shift pattern would be expected than that arising from coordination of the pyridine type nitrogen. A semiquantitative molecular orbital analysis of these results is difficult. Crystalline adducts cannot be obtained for an anisotropic magnetic susceptibility study, so the dipolar contribution cannot be determined. Even if we were to obtain wave functions for the imidazole molecule, it would be necessary to demonstrate that only one isomeric form of the complex exists in solution.

The combination of  $\pi$  delocalization,  $\sigma$  delocalization, and dipolar contributions in a nonaxial system make it difficult to draw definitive conclusions from the shift pattern alone. The line width information presented in the next section strongly suggests coordination at the amine nitrogen. The shift information is consistent with this conclusion.

**Line Width Information.** In the system under investigation, analysis of the  $N$ -MeIm resonance line widths is less complicated than the isotropic shifts and provides strong support for coordination of **1** at the amine nitrogen. In general, paramagnetic NMR line widths can be affected by the two factors, summarized in the following equation:<sup>19</sup>

$$\frac{1}{T_{2M}} = \frac{[4\gamma^2 g^2 \beta^2 S(S+1)]}{3r^6} \tau_c + \frac{[(A_i/h)^2 8\pi^2 S(S+1)]}{3} \tau_e \quad (1)$$

In this equation  $S$  is the total electron spin of the metal ion,  $\gamma_1$  is the nuclear gyromagnetic ratio,  $g$  is the electron magnetic moment in the ion,  $\beta$  is the Bohr magneton,  $(A_i/h)$  is the isotropic shift of the  $i$ th nucleus,  $r$  is the electron-nuclear distance,  $\tau_c$  is the correlation time for tumbling in solution, and  $\tau_e$  is the electronic spin-lattice relaxation time. The first term in eq 1 which usually dominates the observed line widths arises from a dipolar interaction of the nuclear and electron spins and depends on  $1/r^6$ . The second term accounts for the relaxation arising from the coupling of the nuclear and electron spins via

the Fermi contact interaction. The relative importance of the second term will depend upon the magnitude of  $\tau_e$  vs.  $\tau_c$  and  $A_i$ . This second term will be more important in molecules with long  $\tau_e$  and at nuclei with large contact shifts. Even for  $\tau_e = \tau_c$ , with  $r = 3 \text{ \AA}$ , the Fermi contact term will dominate<sup>20</sup> line widths only for contact shifts  $>300$  ppm.

The second term in eq 1 predicts a linear dependence of the line width vs.  $(A_i/h)^2$ . These quantities are plotted for  $N$ -MeIm coordinating to **1** in Figure 5. The nonlinear behavior of the small  $N$ -MeIm isotropic shifts and the relatively sharp NMR signals (conversely the broad ESR signals at  $-160^\circ\text{C}$ ) indicate that  $\tau_e \ll \tau_c$  and that the dipolar term dominates the line widths.

The line widths of all the ring protons and  $N$ - $CH_3$  group in the  $N$ -MeIm complexes of **1** and **2** are tabulated in Table III. The observed line width  $(\delta\nu)_{1/2}$  is related to the relaxation time by  $(\delta\nu)_{1/2} = 1/\pi T_2$ . In the fast-exchange limit,<sup>20</sup>

$$1/T_2 = (P_M/T_{2M}) + (P_A/T_{2A})$$

where  $T_{2M}$  is the relaxation time in the paramagnetic environment (coordinated) and  $T_{2A}$  is the relaxation time in the diamagnetic environment (bulk solvent). The quantities  $P_M$  and  $P_A$  are the probabilities that a given nucleus will be found in the corresponding environment. For a solution which is dilute in paramagnetic species,  $P_A \approx 1$  and we have

$$(1/T_2) - (1/T_{2A}) = (P_M/T_{2M})$$

$1/T_{2A}$  is approximated by  $(1/T_{2A}^0)$  the relaxation time of an equimolar solution of base in the absence of any added paramagnetic complex. It should be noted that the approximation of  $(1/T_{2A}) = (1/T_{2A}^0)$  will be crude in our studies because the concentration of **1** or **2** is on the same order as that of  $N$ -MeIm. The line width of uncoordinated  $N$ -MeIm is likely to be affected by the large concentration of paramagnetic material present.

With  $1/T_{2M}$  governed by the first term in eq 1, ratios of line widths of different nuclei can be solved for corresponding distance ratios. Though precise structural data cannot be obtained, it is evident from the line width data in the presence of **2** that the coordinated  $N$ -MeIm proton distances from the nickel increases in the order  $r_{M-H(2)} < r_{M-H(4)} < r_{M-H(5)} < r_{M-CH_3}$ . Utilizing the approximation of  $1/T_{2A} = 1/T_{2A}^0$  and the solution no. 4 data (to obtain largest line widths) at the three temperatures investigated, we obtain the following distance ratios:

$$r_{M-H(5)}/r_{M-H(2,4)} = 1.27 \quad r_{M-CH_3}/r_{M-H(2,4)} = 1.56$$

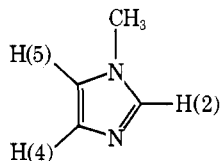
If one assumes the coordination of  $N$ -MeIm to **2** gives rise to a similar metal-ligand geometry as that of  $\text{Co( TPP )} \cdot N$ -MeIm,<sup>21</sup> where the Co-N(3) bond length is found to be 2.157  $\text{\AA}$ , one calculates

$$r_{M-H(5)}/r_{M-H(2,4)} = 1.57 \quad r_{M-CH_3}/r_{M-H(2,4)} = 1.81$$

It is apparent the data are consistent with N(3) (pyridine type) coordinating to the nickel atom of **2**, and if, as suspected,  $(1/T_{2A})$  were larger than  $1/T_{2A}^0$ , the data would be in even closer agreement.

The line width data for the cobalt analogue (**1**) shows that a different ordering of the  $N$ -MeIm proton distance from the metal exists than that found for the analogous nickel complex (**2**). The ordering in this case is  $r_{M-H(4)} > r_{M-H(2)} \sim r_{M-H(5)} \sim r_{M-CH_3}$ . Because the  $[1]/[N\text{-MeIm}]$  ratios utilized are much larger than those of **2** the calculated distance ratios will underestimate the actual ratios by a larger degree than in the case of the nickel(II) complex ( $1/T_{2A} = 1/T_{2A}^0$  is a poorer approximation). The ratios calculated from the line width data in Table III are

Table III



Solution <sup>b</sup>				Solution <sup>b</sup>					
No.	( $\delta\nu$ ) <sub>N-CH<sub>3</sub></sub>	( $\delta\nu$ ) <sub>H(2)</sub> <sup>c</sup>	( $\delta\nu$ ) <sub>H(4)</sub> <sup>c</sup>	( $\delta\nu$ ) <sub>H(5)</sub> <sup>c</sup>	No.	( $\delta\nu$ ) <sub>N-CH<sub>3</sub></sub>	( $\delta\nu$ ) <sub>H(2)</sub> <sup>c</sup>	( $\delta\nu$ ) <sub>H(4)</sub> <sup>c</sup>	( $\delta\nu$ ) <sub>H(5)</sub> <sup>c</sup>
A. Line Widths <sup>a</sup> of <i>N</i> -MeIm Protons in Solutions Containing Co(SMDPT)					4	9.6	8.8	7.0	9.4
$T = 28^\circ\text{C}$					5	13.0	11.6	9.0	12.8
0	1.0	3.4	2.8	3.4	6	15.6	17.6	11.4	17.2
1	1.0	3.6	2.8	3.4	$T = -74^\circ\text{C}$				
2	1.8	4.0	3.0	3.4	0	1.4	3.4	3.8	3.4
3	2.8	5.5	3.2	3.6	1	2.2	3.8	4.2	3.4
4	4.9	6.8	4.2	4.2	2	4.2	5.4	<i>c</i>	<i>c</i>
5	6.7	7.8	5.2	6.8	3	6.8	7.8	6.6	8.0
6	8.3	10.0	6.4	8.8	4	12.4	12.6	8.2	12.6
$T = -5^\circ\text{C}$					5	15.8	16.0	10.0	16.0
0	1.0	4.0	4.0	4.4	6	19.8	20.0	12.0	20.0
1	1.2	4.2	4.2	4.8	B. Line Widths of <i>N</i> -Methylimidazole in Presence of Ni(SMDPT) (See microfilm edition for solution concentrations.)				
2	2.1	4.4	4.4	4.8	$T = 28^\circ\text{C}$				
3	3.5	5.2	<i>c</i>	<i>c</i>	0	1.0	2.0	2.0	2.0
4	6.4	6.8	5.6	7.6	1	1.5		22	5
5	8.6	8.8	7.0	9.2	2	2.5		27	6
6	11.0	10.6	7.8	10.2	3	3.5		45	13
$T = -31^\circ\text{C}$					4	5.0		68	22
0	1.3	3.0	3.6	3.2	$T = 1^\circ\text{C}$				
1	1.7	4.0	3.8	4.0	0	1.0	2.0	2.0	2.0
2	2.8	4.8	4.0	5.0	1	2.0		24	5
3	4.2	5.6	<i>c</i>	<i>c</i>	2	4.5		43	10
4	7.6	8.4	6.2	8.8	3	6.0		75	18
5	10.0	10.6	8.6	10.4	4	9.5		120	29
6	12.5	14.8	11.0	14.4	$T = -25^\circ\text{C}$				
$T = -56^\circ\text{C}$					0	1.5		2.0	2.0
0	1.4	3.6	3.8	3.8	1	3.0		33	6
1	2.2	4.0	3.8	4.0	2	5.5		40	12
2	4.1	5.4	<i>c</i>	<i>c</i>	3	8.5		90	23
3	5.8	6.6	<i>c</i>	<i>c</i>	4	13.0		150	32

<sup>a</sup> ( $\delta\nu$ ) is the full width at half-height, given in hertz at 100 MHz. <sup>b</sup> Solution numbers refer to Figures 1, 2, 3, and 4. <sup>c</sup> H(4) and H(5) resonances overlap too badly to determine line widths. <sup>d</sup> The chemical shifts of *N*-MeIm protons at infinite dilution in cyclohexane have been found to be  $\text{H}_2 = 7.41$ ,  $\text{H}_4 = 7.05$ ,  $\text{H}_5 = 6.88$ ; E. Corradi, P. Lazzarotti, and F. Taddei, *Mol. Phys.*, **26**, 41 (1973). The close agreement in  $\text{CDCl}_3$  allows the assignment as shown (see microfilm edition).

$$\frac{r_{\text{M-H}(4)}}{r_{\text{M-H}(2,5)}} = 1.09 \quad \frac{r_{\text{M-H}(2,5)}}{r_{\text{M-CH}_3}} = 1.03 \quad \frac{r_{\text{M-H}(4)}}{r_{\text{M-CH}_3}} = 1.12$$

Such ratios are consistent only with coordination of the *N*-CH<sub>3</sub> nitrogen to the cobalt. The fact that H(2,5) are closer to the cobalt than H(4) when coordinated to **1** and H(2,4) are closer to the nickel than H(5) in **2** is reinforced by the *N*-CH<sub>3</sub> line widths in both cases. The *N*-CH<sub>3</sub> line widths indicate N(1) (amine) coordination to cobalt and N(3) (pyridine type) coordination to the nickel. Since there is no literature precedent for such a M-N(1) coordination mode, we have not calculated distance ratios because of many possible geometric configurations which can exist [all of which possess ( $r_{\text{M-H}(4)}/r_{\text{M-H}(2,5)}) > 1$ , ( $r_{\text{M-H}(4)}/r_{\text{M-CH}_3}) > 1$ ].

In the coordination of *N*-MeIm to **1**, an equilibrium consisting of N(1) and N(3) donor ligands is a possibility worth considering. Such an occurrence would lead to linear  $\Delta\nu_{\text{N-CH}_3}$  vs. [1] plots as observed in Figure 1. However, if the enthalpy for coordination at N(3) did not equal the enthalpy for coordination at N(1), a nonlinear relationship would result in Figure 2 if there were appreciable concentrations of both types of complexes. The linearity observed implies either comparable enthalpies for binding at both nitrogens or the predominance of adducts coordinated at one site.

It is interesting to note that **1** does not readily coordinate

pyridine. In room temperature, NMR studies of **1** containing a range of [pyridine]/[**1**] of 3.68, 1.58, and 0.85, no shift was observed in any pyridine ring protons. Only upon cooling the solution to 0 °C did a noticeable shift occur in the  $\alpha$ -protons. (For the [pyridine]/[**1**] ratio of 0.85, a shift of 0.4 ppm was observed.)

### Conclusion

NMR chemical shift and line width data for *N*-MeIm upon adduct formation with Co(SMDPT) (**1**) and Ni(SMDPT) (**2**) indicate a different mode of coordination in the two cases. The similarity in chemical shift data of **2** with many previously studied complexes indicate coordination through the imine nitrogen, N(3) of *N*-MeIm. Line width data clearly corroborate this finding. Chemical shift data of *N*-MeIm coordination to **1** show downfield *N*-CH<sub>3</sub> shifts larger in magnitude than any ring proton shifts. The ring protons exhibit both upfield and downfield shifts. This finding is rationalized by coordination of **1** to the N(1) nitrogen of *N*-MeIm, giving rise to  $\sigma$  (downfield shift) delocalization to protons of the *N*-CH<sub>3</sub> group, and a mixture of  $\sigma$  and  $\pi$  delocalization to ring protons. Line width data on this complex strongly support the coordination of N(1) to the cobalt, thus substantiating our previous claim for the ambidentate nature of imidazole. The explanation for

this behavior of the cobalt(II) center is not revealed by these studies, but would require complete thermodynamic data on these systems. The order of complexing ability for the bases reported is certainly an unusual one.

**Acknowledgment.** The authors acknowledge the support of this research by the National Science Foundation.

**Supplementary Material Available:** a tabulation of all chemical shift data of *N*-MeIm and Co(SMDPT) (Table A) and *N*-MeIm and Ni(SMDPT) (Table B) (5 pages). Ordering information is given on any current masthead page.

## References and Notes

- (1) B. S. Tovrog and R. S. Drago, *J. Am. Chem. Soc.*, **96**, 2743 (1974).
- (2) D. Doonan and A. L. Balch, *J. Am. Chem. Soc.*, **97**, 1403 (1975). These authors complained with good reason that "experimental conditions were not described with sufficient precision in our earlier report to enable one to determine if the observed shifts were the result of dilution or complexation. No attempt was made to correspond and obtain this information, and the authors incorrectly concluded that our results in Figures 3 and 4 were carried out in  $\text{CH}_2\text{Cl}_2$  instead of  $\text{CHCl}_3$ . We agree that the ambiguities discussed by Doonan and Balch exist in our earlier system and sought a more straightforward system for demonstrating the ambidentate nature of the imidazole ring system.
- (3) L. Sacconi and I. Bertini, *J. Am. Chem. Soc.*, **88**, 5180 (1966).
- (4) (a) P. L. Orioli, M. DiVaira, and L. Sacconi, *Chem. Commun.*, 300 (1966); (b) M. DiVaira, P. L. Orioli, and L. Sacconi, *Inorg. Chem.*, **10**, 553 (1971).
- (5) G. N. LaMar and L. Sacconi, *J. Am. Chem. Soc.*, **89**, 2282 (1967).
- (6) I. Bertini, L. Sacconi, and G. P. Speroni, *Inorg. Chem.*, **11**, 1323 (1972).
- (7) Observed line widths in **1** are larger than those in **2** due to longer  $\tau_e$ . It is not known if the "doubling" is obscured at higher temperatures because of the larger line widths or if a rapid exchange between different geometries is slowed at low temperatures.
- (8) W. D. Perry and R. S. Drago, *J. Am. Chem. Soc.*, **93**, 2183 (1971).
- (9) For a tabulation of all chemical shift data upon coordination to *N*-MeIm, see microfilm edition.
- (10) R.-M. Claramunt, J. Elguero, and R. Jacquier, *Org. Magn. Reson.*, **3**, 595 (1971).
- (11) R. Cramer and R. S. Drago, *J. Am. Chem. Soc.*, **92**, 66 (1970).
- (12) D. Doddrell and J. D. Roberts, *J. Am. Chem. Soc.*, **92**, 6839 (1970).
- (13) W. DeW. Horrocks and D. L. Johnston, *Inorg. Chem.*, **10**, 1835 (1971).
- (14) M. Wicholas, R. Mustacich, B. Johnson, T. Smedley, and J. May, *J. Am. Chem. Soc.*, **97**, 2113 (1975).
- (15) R. G. Sievers, Ed., "Nuclear Magnetic Resonance Shift Reagents", Academic Press, New York, N.Y., 1973.
- (16) I. Bertini and D. Gatteschi, *Inorg. Chem.*, **12**, 2740 (1973).
- (17) R. J. Fitzgerald and R. S. Drago, *J. Am. Chem. Soc.*, **90**, 2523 (1968).
- (18) R. J. Fitzgerald and R. S. Drago, *J. Am. Chem. Soc.*, **89**, 2879 (1967).
- (19) See T. J. Swift in "NMR of Paramagnetic Molecules", W. DeW. Horrocks, Jr., and G. N. LaMar, Ed., Academic Press, New York, N.Y., 1973.
- (20) See C. Langford and T. S. Stengle in ref 19.
- (21) W. R. Scheidt, *J. Am. Chem. Soc.*, **96**, 90 (1974).

# On the Photochemical Substitution Reactions of Hexacoordinated Transition Metal Complexes

L. G. Vanquickenborne\* and A. Ceulemans

Contribution from the Department of Chemistry, University of Leuven, Celestijnenlaan 200F, B-3030 Heverlee, Belgium. Received April 12, 1976

**Abstract:** The two empirical rules of Adamson were the first attempt to provide a qualitative description of the photochemical substitution reactions of transition metal compounds. It is our purpose (i) to offer an alternative to Adamson's rules (ii) to rationalize the photochemistry by means of a simple model. The model is based on a ligand field approach where the contribution of each ligand is additive in the orbital energy. In a  $D_{4h}$  environment, this contribution depends on whether the ligand is in axial or equatorial position. In order to account for the bonding interactions, it is assumed that the ligand basis orbitals are stabilized to the same extent that the metal orbitals are destabilized. Energy expressions have been derived for  $d^3$  and  $d^6$  systems, in each case for  $\sigma$ -donor,  $\pi$ -donor, and  $\pi$ -acceptor ligands. Using the strong field wave functions, the relevant bond energies in the photoactive states can be calculated. Comparison with the available experimental data on Cr(III) and Co(III) complexes yields a very satisfactory agreement between theory and experiment.

Irradiation of transition metal complexes in the ligand field part of their spectrum gives rise to a strongly enhanced substitution activity. It is well known that the photoexcitation induces the exchange of ligands from the primary coordination sphere with solvent molecules, or with free ligands from the solution.<sup>1,2</sup>

Most of these photochemical substitution reactions of octahedral complexes seem to be governed by two rules, first formulated by Adamson:<sup>3</sup> (i) the leaving ligand is situated on the axis characterized by the weakest ligand field; (ii) of the two ligands situated on the labilized axis, the leaving ligand is the one exhibiting the strongest ligand field.

It is the purpose of this note to formalize in a very simple way the chemical intuition behind Adamson's empirical rules. With this object in view, a number of theoretical models have already been introduced and the groundwork has been laid for understanding ligand field photochemistry.<sup>4-11,28</sup> Although the present approach will be utterly unsophisticated, it goes beyond the existing models in its way of predicting the labilized ligand without needing extensive molecular orbital calculations.

## Description of the Model

Consider a metal ion in an octahedral environment with the six ligands on the three coordinate axes. Consider a one-electron problem, with a metal basis set consisting of the five  $d$  orbitals. Within the framework of an additive angular overlap model, one has to specify two parameters,  $\sigma_L$  and  $\pi_L$ , for each ligand  $L$ .<sup>12-14</sup> The relevant perturbation matrix is shown in eq 1. While the general complex with six different ligands has no symmetry whatsoever, the matrix is seen to correspond to at least  $D_{2h}$  symmetry. Indeed, the parameters always appear as sums of pairs on the same axis, for instance  $\sigma_z + \sigma_{-z}$ ,  $\pi_y + \pi_{-y}$ , etc. These sums can obviously be replaced by  $2\bar{\sigma}_z = (\sigma_z + \sigma_{-z})$ ,  $2\bar{\pi}_y = (\pi_y + \pi_{-y})$ , etc., so that one is left with six effective, average parameters, one ( $\bar{\sigma}$ ,  $\bar{\pi}$ ) set for each axis. If the perturbation along the three axes is equal, the effective (holoheder) symmetry is  $O_h$ ; if two axes ( $x$  and  $y$ ) are perturbed in the same way, but different from the third one ( $z$ ), the effective symmetry is  $D_{4h}$ ; if they are all different, the holoheder symmetry<sup>15</sup> is still at least  $D_{2h}$ . In the latter case,